Effect of Starting Particle Size and Vacuum Processing on the $YBa_2Cu_3O_x$ Phase Formation

G. S. Grader,* P. K. Gallagher, and D. A. Fleming

AT&T Bell Laboratories, Murray Hill, New Jersey 07974

Received September 28, 1989

The solid-state route using Y_2O_3, $BaCO_3$, and CuO to synthesize the $YBa_2Cu_3O_7$ superconductor requires an effective and complete decomposition of the carbonate. We have found that by reducing starting particle size, improving the mixing, and vacuum processing most of the $BaCO_3$ decomposes in the 550–600 °C range. The enhanced decomposition is lower by >150 °C than the expected $BaCO_3$ decomposition temperature under similar conditions. The cause of this enhancement was found to be a reduced form of CuO that reacts with the $BaCO_3$ to form $BaCu_2O_2$. Upon oxidation, the 1-2-3 phase forms only from the reacted $BaCO_3$, even at temperatures below 650 °C. Virtually complete conversion to the 1-2-3 phase occurs by vacuum processing at ~750 °C followed by oxidation at ~800 °C.

Introduction

In the processing of most ceramics it is well recognized that the size of the starting particles and their distribution is of utmost importance in determing the properties of the final body. For example, smaller particles, which are more reactive, can sinter at lower temperatures than larger particles. The conventional solid-state route to the $YBa_2Cu_3O_7$ (1-2-3) superconductor utilizes Y_2O_3, $BaCO_3$, and CuO as starting materials. The initial particle size can be reduced by grinding or ball milling or by the use of coprecipitation of the oxalates[1,2] or hydroxycarbonates.[3,4] All the preparation routes above present the issue of $BaCO_3$ decomposition. It is important that the carbonates decompose at relatively low temperatures, preferably before the 1-2-3 superconducting phase has formed. By doing so, the entrapment of $BaCO_3$ in the dense sintered body[5] is avoided. When the carbonates are not fully decomposed, they may be incorporated into the 1-2-3 phase.[6] It has been well-known that the decomposition of $BaCO_3$ can be reduced by ~100 °C at a low pressure of oxygen and CO_2.[7] Following this notion it has been shown that the rate of 1-2-3 phase formation can be enhanced at low P_{CO_2} and P_{O_2}, in vacuum, while the temperature of phase formation is lowered.[2,8] The objective of this work was therefore to study the effect of starting particle size and vacuum processing on the 1-2-3 phase formation.

In the present work we have found that the rate of $BaCO_3$ decomposition can be induced at still lower temperatures in a mixed oxide system, by the presence of a reduced form of CuO. The enhanced $BaCO_3$ decomposition is accompanied by the formation of $BaCu_2O_2$.[9] This enhancement, occurring in the 550–620 °C range, is a strong function of the initial particle size. As expected, the largest enhancement is obtained for the most intimately mixed, finest powder. An analogous behavior in the $Y_2(CO_3)_3$ analogue was not found because this carbonate decomposes before CuO is reduced. The 1-2-3 phase in the present study starts forming below 650 °C. A major amount of 1-2-3 phase occurs at 750 °C by an initial heating under vacuum followed by a soak in oxygen, while near complete conversion occurs at 800 °C.

Table I. Cumulative Particle Size of Mixed Y_2O_3, $BaCO_3$, and CuO as a Function of Ball Milling Time

	cumulative particle size, μm			
milling time, h	95%	90%	50%	10%
1	12.0	7.5	1.60	0.72
3	7.0	5.0	1.70	0.86
6	6.0	4.2	1.60	0.77
16	4.8	3.5	1.53	0.74
32	3.7	3.0	1.25	0.70

Experimental Procedure

Samples for this study were prepared from Y_2O_3, $BaCO_3$, and CuO. The precursor powders were assayed by thermogravimetry to correct for the adsorbed H_2O and CO_2. Weighted amounts of raw powders were then ball milled in propanol for various times (ranging from 1 to 32 h) by using a zirconia media. The powder was then vacuum filtered, dried, and sieved through 100-mesh screen.

The particle size distribution of the powder was measured with a Micromeritics 5000D X-ray sedigraph. This instrument determined the particle size distribution by measuring the rate of sedimentation of particles in suspension. The suspension was prepared by dispersing 0.9 g of superconducting powder in 30 cm^3 of A-11 sedisperse, a commercial dispersant with a density of 0.747 g cm^{-3} and a viscosity of 1.35 cP at 32 °C. To ensure that the powder was well dispersed, the suspension was placed in an ultrasonic bath for approximately 1 h. The data were automatically presented as a cumulative percent distribution in terms of an equivalent spherical diameter between 50 and 0.2 μm.

Weight loss during heating was measured by thermogravimetry (TG) using a Perkin-Elmer system 7 thermal analyzer with their standard furnace and Pt sample pan. The heating rate was 1 °C min^{-1} in a flow of O_2 (~50 mL min^{-1}). Mass spectrometric evolved gas analysis (EGA) was performed using a customized system[10] and TECKNIVENT software. The vacuum was $\sim 2 \times 10^{-7}$ Torr after outgassing at room temperature. The sample was then heated at 20 °C min^{-1} in a small Pt crucible, and the pressure rose to $\sim 2 \times 10^{-5}$ Torr at the maximum decomposition rate. Nominally, 6-mg samples were used for 123 mixtures, and appropriately

(1) Kameko, K.; Ihere, H.; Hirabayashi, M.; Terada, N.; Sonzaki, K. *Jpn. J. Appl. Phys.* **1987**, *26*, L734.
(2) Gallagher, P. K.; Fleming, D. A. *Chem. Mater.*, previous paper in this issue.
(3) Bunker, B. A.; et al. In *Better Ceramics through Chemistry III*; Brinker, C. J., et al., Eds.; Materials Resource Society: Pittsburgh, PA, 1988; pp 373–384.
(4) Morgan, D., Maric, M., Richardson, J. T. and Luss, D., to be published.
(5) Shaw, T. M.; Dimos, D.; Duncombe, P. R. *1989 Am. Ceram. Soc. Annu. Mtg.*, Apr 23–27, Indianapolis, IN.
(6) Roth, R. S.; Rawn, C. J.; Beech, F.; Whitler, J. D.; Anderson, J. O. *Research Update, 1988: Ceramic Superconductors II*; Yan, M. F., Ed; American Ceramics Society: Columbus, OH, 1988; pp 13–26.
(7) Basu, T. K.; Searcy, A. W. *J. Chem. Phys.* **1976**, *80*, 1889.
(8) Lay, K. W. *J. Am. Chem. Soc.* **1989**, *72*, 696.
(9) Teske, C. L.; Mueller-Buschbaum, H. *Z. Naturforsch B* **1972**, *27*, 296.
(10) Gallagher, P. K. *Thermochim. Acta* **1978**, *26*, 175.

0897-4756/89/2801-0665$01.50/0

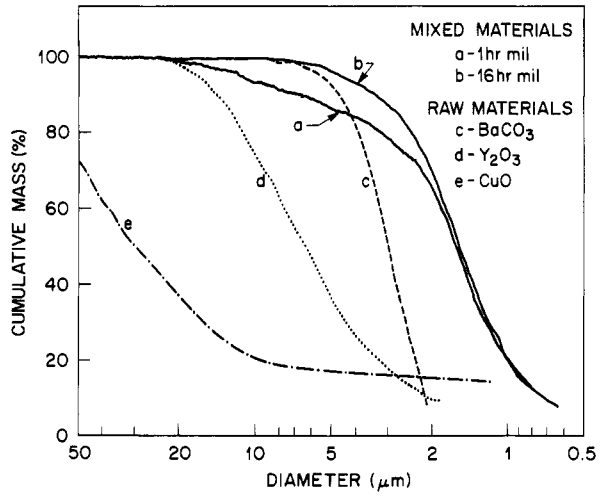

Figure 1. Cumulative particle mass vs the particles diameter for Y_2O_3, $BaCO_3$, and CuO ball milled for 1 and 16 h.

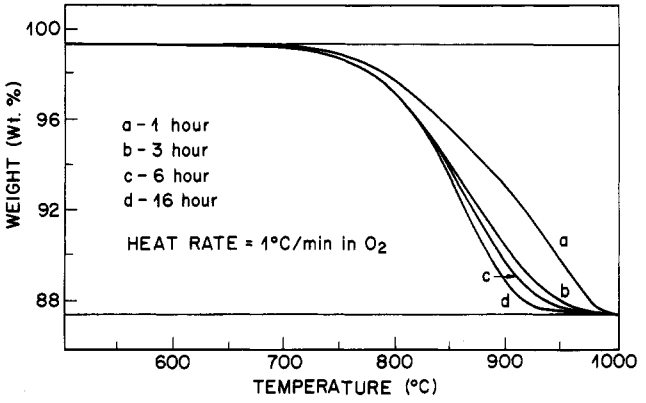

Figure 2. Weight loss of Y_2O_3, $BaCO_3$, and CuO during 1-2-3 phase formation for samples milled for 1–16 h. The heating conditions are 1 °C/min in O_2.

smaller amounts for the pure CuO and $BaCO_3$ experiments.

Vacuum processing was carried out in a vertical, closed end, fused quartz tube, into which a small Al_2O_3 crucible (containing the sample) was lowered. The tube was connected to a mechanical pump that provided a pressure of $\sim 5 \times 10^{-6}$ atm. The temperature was monitored below the crucible. Samples were usually quenched from the high temperature by moving the fused quartz tube out of the furnace (still under vacuum) and forcing cold air over the tube. The temperature of the sample drops to <100 °C in <2 min. The X-ray pattern of the processed powders was measured with a Phillips automated powder difractometer, using Cu Kα radiation.

Results and Discussions

A variety of starting particle sizes were obtained by ball milling for various times. The cumulative particle sizes at 95%, 90%, 50%, and 10% cutoffs are shown in Table I. In Figure 1 the actual sedigraph curves for the 1- and 16-h milling times are shown (traces a and b, respectively). As seen from trace a, the initial size distribution includes a distinct fraction of large particles. As shown, the starting CuO aggregate size is much larger than the $BaCO_3$ and Y_2O_3, and the effect of the milling is partly to break up the aggregates, thereby producing a narrower size distribution.

The resulting TG curves for the samples heated in O_2 at 1 °C min^{-1} are shown in Figure 2. It is clear that the rate of reaction increases with smaller particles. For trace d in Figure 2 the conversion (based on the expected weight loss) is 95% complete at ~900 °C. It was also found that the TG trace for the powder milled for 32 h was virtually

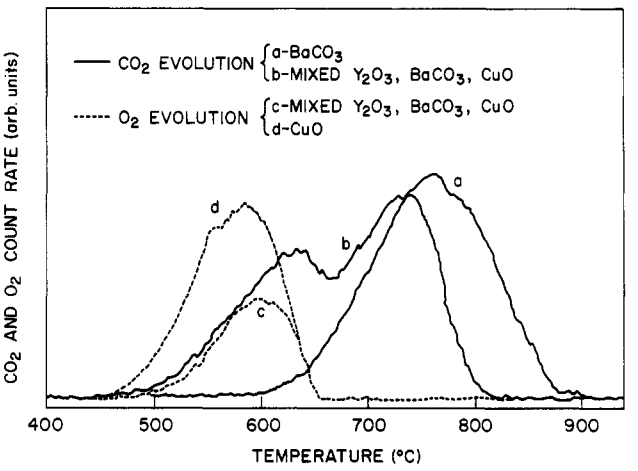

Figure 3. Evolved gas analysis of $BaCO_3$ (a), mixed oxides (b, c), and CuO (d) as a function of temperatures. Curves a and b show the CO_2 evolution, while curves c and d show the O_2 evolution.

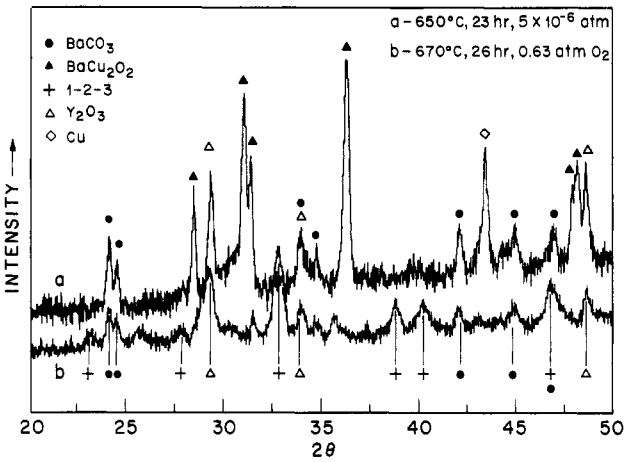

Figure 4. X-ray pattern of the 32-h milled sample after 23 h at 650 °C in vacuum (a), followed by exposure to O_2 for 26 h at 670 °C (b).

identical with that of the powder milled for 16 h.

The decomposition of the precursors was followed by EGA. Figure 3 (trace a) shows the EGA of CO_2 for $BaCO_3$ heated at 20 °C min^{-1}. The trace shows a broad single peak with a maximum around 780 °C, consistent with the decomposition temperature published elsewhere.[7] Also shown in Figure 3 (trace b) is the EGA of CO_2 in the mixed oxide system (Y_2O_3, $BaCO_3$, and CuO). Aside from the shift to lower temperatures, the marked difference between the two plots is the emergence of a lower temperature peak around 625 °C, indicating an earlier decomposition of $BaCO_3$. To elucidate the cause of the earlier decomposition, the evolution of O_2 was tracked simultaneously with that of CO_2. As shown in Figure 3 (trace c) the oxygen evolution near 600 °C correlates with the first peak in the $BaCO_3$ decomposition. To find out the oxygen source, EGA of CuO and Y_2O_3 were measured separately. As shown in trace d, it was found that CuO lost oxygen near 600 °C, indicating a reduction of CuO. The presence of Cu is confirmed by the X-ray data shown in Figure 4 for a mixed oxide sample that had been held at 650 °C for 23 h at a pressure of $\sim 5 \times 10^{-6}$ atm.

The enhancement of the $BaCO_3$ decomposition by the reduced form of CuO is found to depend strongly on the starting particle size. A plot of the O_2 and CO_2 evolution from the powders milled for 1, 6, 16, and 32 h is shown in Figure 5. After 1 h of milling, the CuO particles were still

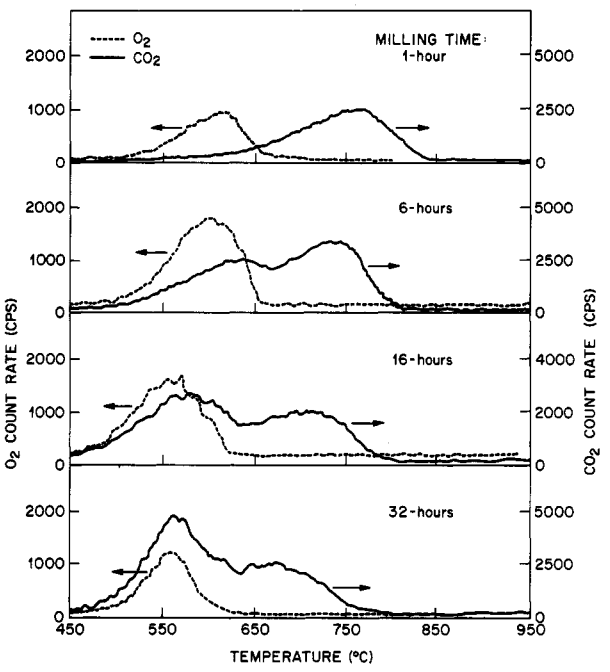

Figure 5. Evolved gas analysis of samples milled for 1, 6, 16, and 32 h as a function of temperature. The O_2 and CO_2 evolutions are tracked simultaneously.

much larger than the $BaCO_3$, so that the contact between them is poor. Consequently no enhancement in the $BaCO_3$ decomposition is observed. As the milling time is increased and the particles come into closer contact, an increasing amount of $BaCO_3$ decomposes at the lower temperature. For 16 and 32 h of milling most of the $BaCO_3$ decomposes at the lower temperature, as evident from the relative area under the peaks at 550 and 700 °C. The effect may be an extension of the Hedvall effect,[11] where a material undergoing a phase transition is more reactive due to increased defect concentration. In the present case, however, the CuO is reducing rather than undergoing a phase transition. Another phenomenon that may be related to the present effect is the enhanced solid reactivity following a mechanochemical treatment.[12]

It is also apparent that the action of reduced CuO on $BaCO_3$ leads to the formation of the $BaCu_2O_2$ phase. This was indicated by comparison of the X-ray diffraction pattern for a sample milled for 1 h and fired at the same conditions as those in Figure 4a. Even though the CuO was reduced, much less $BaCu_2O_2$ was formed. In addition to the emergence of a $BaCO_3$ decomposition peak at lower temperature, the second effect of reducing the particle size is to lower the overall reaction temperature. The CuO and first $BaCO_3$ decomposition peaks shift from ~620 to 550 °C, while the second $BaCO_3$ decomposition peak shifts from 780 to ~700 °C. This trend is expected as the higher surface area and defects induced by grinding make the finer powder more reactive.

After exposure of the sample of Figure 4a to oxygen, a significant amount of the 1-2-3 phase is present. However, it is apparent that the portion of $BaCO_3$ and Y_2O_3 that did not decompose in the vacuum step does not react during the oxidation stage at these temperatures. This is consistent with the 1-2-3 phase forming from the $BaCu_2O_2$ and copper phases, which disappear completely after the oxidation. Figure 6 shows the X-ray pattern of samples held

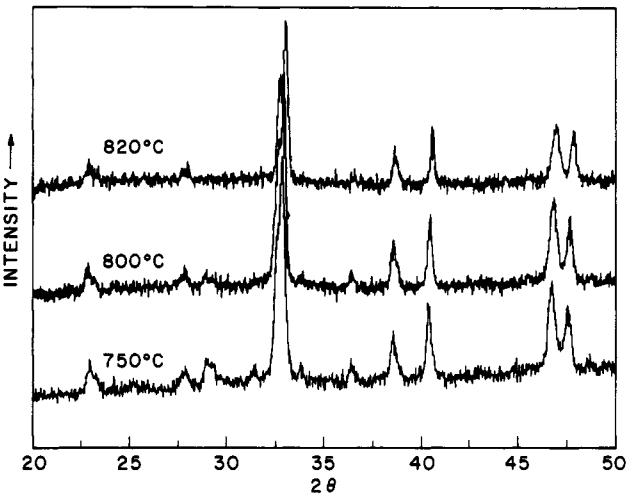

Figure 6. X-ray pattern of 32-h milled samples fired at 750 °C in vacuum followed by oxidation at (a) 750, (b) 800, and (c) 820 °C.

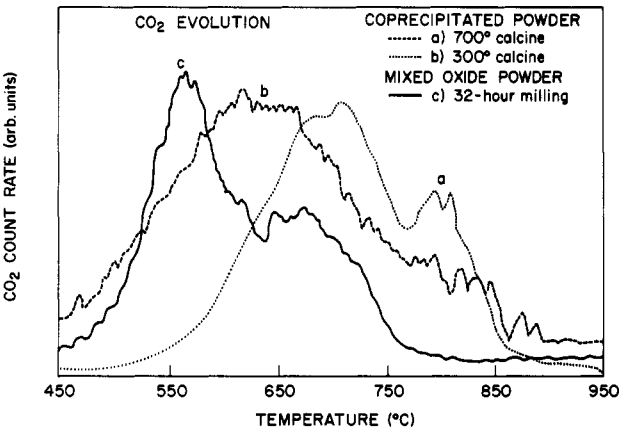

Figure 7. Evolved gas analysis of CO_2 as a function of temperature for an oxalate coprecipitated sample calcined at (a) 300 and (b) 700 °C, and (c) for a 32-h milled sample.

in vacuum at 750 °C followed by oxidation at 750, 800, and 820 °C. The $BaCO_3$ has totally decomposed, while the conversion to the 1-2-3 phase is virtually complete.

It is worthwhile noting that the results obtained here via conventional processing are comparable to those obtained from coprecipitated samples. Figure 7 compares the CO_2 evolution of the sample milled for 32 h (Figure 4) to the corresponding evolution from an oxalate coprecipitated samples.[2] Traces a and b show the EGA of oxalate samples calcined at 300 and 700 °C, respectively. As in Figure 5, the difference between traces a and b results from a larger grain size in b due to the higher calcining temperature. As in the milled samples, the fine CuO grains of the coprecipitated sample enhance most of the $BaCO_3$ breakup; however the leftover $BaCO_3$ decomposes at a higher temperature than the milled samples.

Conclusions

It has been shown that in conventionally prepared 1-2-3 powder (from Y_2O_3, $BaCO_3$, and CuO), the $BaCO_3$ decomposition can be induced at ~550 °C by the presence of reduced CuO which forms at low pressures (~10^{-5} atm). To obtain a high degree of early $BaCO_3$ decomposition, a good contact between the CuO and $BaCO_3$ is required. Such a contact is possible only when the initial coarse CuO particles are mechanically broken down or when coprecipitated powders that have initially fine and intimately mixed grains were used. Results using the two techniques

(11) Hedvall, J. A. *Chem. Rev.* **1984**, *15*, 139.
(12) Butyagin, P. Yu. *React. Solids* **1985**, *1*, 345.
(13) Cava, R. J.; Krajewski, J. J.; Peck, Jr., W. F.; Batlogg, B.; Rupp, Jr.; L. W., submitted for publication.

are shown to be comparable.

It is possible to fully decompose the $BaCO_3$ in the 700–750 °C range by using vacuum processing with small initial particles. When this powder is then exposed to oxygen at ~750 °C, a majority of the 1-2-3 phase is obtained. Virtually complete conversion to the 1-2-3 phase is obtained at 800 °C.

Acknowledgment. We thank H. M. O'Bryan for helpful discussions.

Synthetic Approaches to Head-to-Tail Linked Azo Dyes for Nonlinear Optical Applications

M. L. Schilling and H. E. Katz*

AT&T Bell Laboratories, Murray Hill, New Jersey 07974

Received July 25, 1989

Two pathways for the synthesis of dipolar, main-chain azo dye oligomers were investigated. The first involves amide coupling of an *N*-arylpiperazine with a cyanocinnamic acid terminated azo dye, while the second depends upon Knoevenagel condensations of piperazinamides of cyanoacetic acid with (arylazo)benzaldehydes. The amide coupling was successful in the case of *N*-phenylpiperazine but failed with ((arylazo)phenyl)piperazines. The Knoevenagel condensation was more general and made possible the syntheses of a dimeric azo dye and an oligomeric azo dye mixture with the desired connectivity. The principal molecular moments of the chromophores in these oligomers, when in extended conformations, are significantly additive so that we might expect poled polymeric materials containing these oligomers to exhibit larger hyperpolarizabilities than would materials containing analogous, monomeric chromophores. Dipole moment measurements on the dimer and on models of its two "halves" confirmed this additivity.

Introduction

Second-order nonlinear optical materials consisting of azo dyes poled in polymer matrices have been considerably advanced[1] since the prototypical Disperse Red–1-poly(methyl methacrylate) (DR1–PMMA, 11-PMMA) system was first reported.[2] The use of cyanovinyl groups as electron acceptors, resulting in increased values of β and μ,[3] and corona poling, which increases the orienting electric field, has led to materials with electrooptic figures of merit comparable to those of lithium niobate.[1a,c] Furthermore, some of these materials have been shown to exhibit useful activity in devicelike structures.[4]

The first dye–polymer materials fabricated for nonlinear optics were two-component solutions.[2,5] Because of the molecular motion of the solute dyes, even in the glassy state, much of the orientation imparted to the dyes during poling is lost in a matter of days to weeks. The decay in orientation, and thus in the nonlinear optical properties, has been mitigated in more recent materials by covalent attachment of the chromophores to the polymer host, as well as by increasing the length of the chromophoric molecules.[1b]

The highest order parameter achieved so far with the azo dyes currently employed is about 20% so that relatively little of the cumulative second-order nonlinear susceptibility of the individual dye moieties is translated into the bulk hyperpolarizability. One means of increasing the poling-induced order while keeping the chromophores covalently bound to long, polymeric molecules would be to assemble the active species in a head-to-tail fashion so that their dipole moments would necessarily add, and each chromophore would be oriented by the electric field acting on the larger cumulative dipole moment. A detailed theoretical treatment of such an approach has recently appeared, along with initial experimental results.[6] For a chain of chromophores whose β and μ vectors are almost coincident with the vectors connecting the points of attachment of the respective monomer units to the chain, the degree of orientational enhancement possible is proportional to the average $n \cos^2 \theta$, where θ is the angle of those vectors with respect to the overall chain direction and n is the degree of polymerization. A polymer that is "stretched out" so that the dipolar chromophores point from the beginning of the chain to the end will display a large enhancement, while one in which the chromophores point in uncorrelated directions will show a negligible enhancement or even a diminution of effective dipole moment per chromophore.

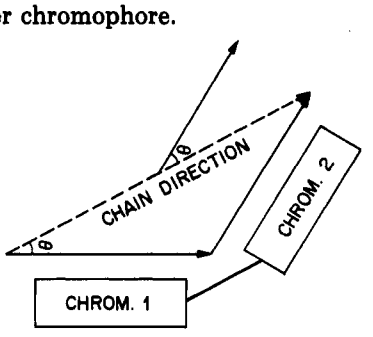

(1) (a) Singer, K. D.; Kuzyk, M. G.; Holland, W. R.; Sohn, J. E.; Lalama, S. J.; Comizzoli, R. B.; Katz, H. E.; Schilling, M. L. *Appl. Phys. Lett.* **1988**, *52*, 1800. (b) Hampsch, H. L.; Yang, J.; Wong, G. K.; Torkelson, J. M. *Macromolecules* **1988**, *21*, 526–528. Hampsh, H. L.; Yang, J.; Wong, G. K.; Torkelson, J. M. *Polym. Commun.* **1989**, *30*, 40. (c) Pantelis, P.; Hill, J. R.; Oliver, S. N.; Davies, G. J. *Br. Telecom Technol. J.* **1988**, *6*, 5–17.

(2) Singer, K. D.; Sohn, J. E.; Lalama, S. J. *Appl. Phys. Lett.* **1986**, *49*, 248–50.

(3) Katz, H. E.; Singer, K. D.; Sohn, J. E.; Dirk, C. W.; King, L. A.; Gordon, H. M. *J. Am. Chem. Soc.* **1987**, *109*, 6561–3.

(4) Thackara, J. I.; Lipscomb, G. F.; Stiller, M. A.; Ticknor, A. J.; Lytel, R. *Appl. Phys. Lett.* **1988**, *52*, 1031–3.

(5) (a) Meredith, G. R.; VanDusen, J. G.; Williams, D. J. Nonlinear Optical Properties of Organic and Polymeric Materials. *ACS Symp. Ser.* **1983**, *233*, 109–133. (b) Marks, T. J. Presented at the 193rd Meeting of the American Chemical Society, Denver, CO, April, 1987. (c) Stamatoff, J. B.; et al. *Proc. SPIE* **1986**, *682*, 85–92.

0897-4756/89/2801-0668$01.50/0